HTD-Vol. 206-1, Topics in Heat Transfer Volume 1
ASME 1992

VISUALIZATION OF HIGH-FREQUENCY THERMO-FLUID PHENONEMA USING REAL-TIME HOLOGRAPHIC INTERFEROMETRY AND NUMERICAL ANIMATION

D. Majumdar and C. H. Amon
Carnegie Mellon University
Pittsburgh, Pennsylvania

C. V. Herman and F. M .yinger
Technical University of Munich
Munich, Germany

B. B. Mikic
Massachusetts Institute of Technology
Cambridge, Massachusetts

Abstract

A combined numerical and experimental visualization of fast-evolving thermo-fluid phenomena in oscillatory viscous flows is presented for geometries composed of periodically interrupted surfaces such as those encountered in compact heat exchangers. The spatially-periodic, geometric inhomogeneities induce traveling waves that produce self-sustained oscillations. The oscillatory thermal phenomena are visualized experimentally by means of real-time holographic interferometry. The transient temperature fields are recorded using high-speed cinematography. Digital image processing was implemented in the evaluation of the interferogram sequences. The numerical approach is based on direct numerical simulation of the unaveraged Navier-Stokes and energy equations. The high volume of numerical data generated on the Cray Y-MP is presented both in computer-aided animation form and as instantaneous plots.

Introduction

The goal of large-scale simulations and experiments in computational science is to obtain a quantitative and physical understanding of the phenomenon being investigated. Trying to observe patterns created by fluid flowing over or around an object is a challenging task. A key component in the process of confronting this problem is visualization which provides access to new areas of exploration and enables us to study observed phenomena in greater detail and thus gain a better understanding of the phenomena of fluid mechanics. Visualization can be either experimental or computational.

Experimental flow visualizations may involve flows in wind or water tunnels, where classical visualizing techniques such as smoke injection, dye advection and time exposure photographs are generally used. Additional flow visualization techniques are Schlieren methods, laser sheet illumination, stroboscopic illumination and injection of tracers sensitive to fluid properties such as temperature. Therefore, different visualization techniques are available which help us gain a better insight into a physical phenomenon (Van Dyke, 1982 and Merzkirch, 1987). Among these techniques, the field measurement approach is very attractive for quantitative analysis of complex physical processes, since it provides information on the whole flow field at a certain time. However, the applications of field measurements analyses have been very limited due to the complexity of the extraction of quantitative data from the images, which is a tedious, time-consuming procedure when performed manually. The availability of modern digital image processing equipment has enabled a relatively fast and easy analysis of visualization images. As a result of the digital image processing procedure, the extracted data are visualized in a form which emphasizes the important features of the investigated phenomenon. The flow structure may be shown in three-dimensional graphs (Hesselink, 1988). The temperature fields and corresponding heat transfer data can be obtained by evaluating the interferometric fringe pattern which can be presented graphically as a function of the spatial coordinates (Herman and Mayinger, 1991). Most of the applications of digital image processing reported in the literature are concerned with the analysis of individual images of stationary phenomena or the instantaneous state of a nonstationary process as described, for example, by Hunter and Collins (1987) and Osten et al. (1987).

However, in practical applications, the processes are generally nonstationary, and the analysis of the temporal evolution of the phenomenon is required for its thorough understanding. Very often, the complete information contained in a single image is not necessary for quantitative analyses. The temporal development of certain events and the motion of certain characteristic points in space are what the investigator is seeking. Therefore, a complete analysis may be performed for a few selected images at characteristic time instants.

The applications of the computer graphics to flow visualization are relatively new and involve the use of

modern high-performance computer graphics techniques to depict and project the resulting data, although the computer system requirements for unsteady flow visualizations are quite substantial. These graphics techniques not only enable visual interpretation of the details of the numerically generated flow fields but also allow comparisons between numerical solutions and visual representations of the actual flow obtained by experimental means. An early paper on flow visualization in computational fluid dynamics discussed the algorithms needed for flow visualization (Buning and Steger, 1985). These algorithms can be broadly classified into two types: the Eulerian approach, of which contour lines and contour surfaces are typical examples and the Lagrangian approach, which can be exemplified by particle tracing. Bareta (1991) discussed a general method to obtain three-dimensional flow visualization using velocity components to track particles for the case of a single jet impinging on a flat plate.

In the present work, we are concerned with the flow in a pair of channels separated by a thick wall with open slots nearly as long as the solid part of the wall. These slots enable the two streams to interact, and the two channels can be said to be communicating with each other. This particular geometry finds its application in compact heat exchangers because of the associated thin thermal boundary layers which result in substantial heat transfer enhancement. Above a critical Reynolds number, flows in this geometry bifurcate to a time-periodic, self-sustained oscillatory state, and the associated thermo-fluid phenomena become extremely fast.

To capture these fast-occurring phenomena, we have developed both experimental and numerical tools that allow us to analyze the complex physics of oscillatory viscous flows, in particular, the thermal phenomena in communicating channels. The real-time method of holographic interferometry was selected for experimental visualization as it enables visualization and quantitative measurement of temperatures with high-spatial and temporal resolutions without disturbing the investigated physical phenomena. A modern digital image processing technique is implemented in the analysis of transient temperature fields recorded as high-speed image sequences. A procedure, which is convenient for the evaluation of transient phenomena from a sequence of interferograms recorded at different time instants, is discussed. Numerical animations were resorted to, based on an Eulerian framework, to analyze the problem from the computational viewpoint. Massive amount of data was generated and processed with the help of high-resolution graphics techniques. The numerical results are presented as computer-animated films as well as instantaneous plots.

Experimental and Numerical Methods of Study

The communicating-channels geometry, shown in Fig. 1, is composed of a succession of colinear plate segments aligned parallel to the flow. The experimental test section is rectangular, and ten heated plates, forming the interrupted surface, are aligned in the mid-plane of the duct constituting the two communicating channels. The working fluid is air and the measurements are performed on the ninth plate as the flow becomes periodically fully developed by the time it reaches this plate. The ratio of channel height to the width in the spanwise direction is 1:15 which essentially renders the flow and temperature fields two-dimensional. Since the method selected for our experimentation, holographic interferometry, involves integration in the spanwise direction, the requirement for two-dimensional temperature fields is important for accurate reconstruction of temperatures. A detailed description of the setup can be found in Amon et al. (1991).

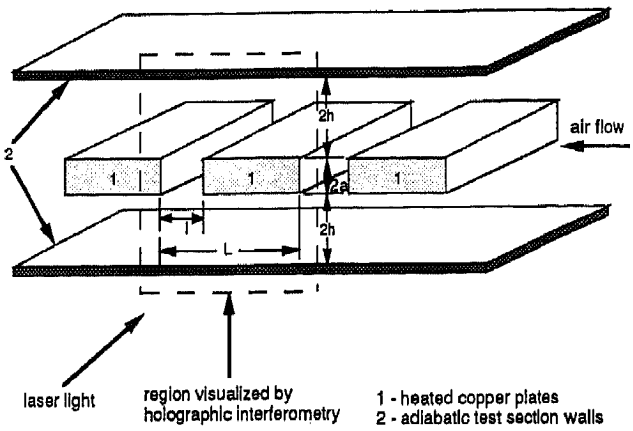

Fig. 1 Schematic of the communicating-channels geometry: plate spacing, l=0.015m; separation distance between channels, 2a=0.005m; periodicity length, L=0.04m and channel height, 2h=0.01m.

The flow in the communicating channels is simulated numerically by solving the time-dependent Navier-Stokes and energy equations for Newtonian, incompressible, two-dimensional flows. Natural convection, viscous dissipation and variation of thermal properties are neglected in the formulation of the problem. The velocity boundary conditions are Dirichlet on rigid walls and periodic in the streamwise direction (Fig. 1). The thermal boundary conditions are uniform heat flux on the interrupted plates with adiabatic top and bottom walls. The numerical approach followed here involves direct numerical simulation of the unaveraged Navier-Stokes and energy equations employing the spectral element method (Patera, 1984). Details of the mathematical formulation and the numerical method of solution are presented in Amon et al. (1991).

Extraction of Nonstationary Data from Interferograms

Interferograms contain continuous two-dimensional information on the field variable (in our investigations, the temperature field) coded as irradiance distribution in the form of fringes. The existence of visual information is one of the important advantages of this measurement technique. However, considering the large amount of information contained in a single interferogram, the extraction of quantitative data and the data reduction procedure have always presented a serious problem and limited the applications of interferometry. Interferograms are usually evaluated by accurately measuring the location of fringe irradiance minima and maxima with a micrometer under a microscope combined with a photometer, and the data obtained in this way are evaluated with a computer.

The problem becomes even more pronounced in transient real-time interferometric measurements where several hundreds or thousands of images are recorded for a single state. Temperature fields at a certain time instant are evaluated in a similar fashion as the steady-state images. The time history of the event is obtained by first identifying the event in a sequence of interferograms and then analyzing the change in the event by comparing the interferograms in the investigated sequence. Thus, in the analysis of transient phenomena, the difficulty of comparing individual images is added to the original data reduction problem. In such situations, a manual evaluation is extremely tedious due to the prevalence of available data. The problem is further intensified by the simultaneous requirement of visualizing at least two interferograms from the sequence to recognize a change between individual exposures. This calls for new solutions in the evaluation process.

The field of holographic interferometry has profited strongly from the rapid development of computer technology in the past decade. The development of accessible powerful computers has enabled the implementation of digital image processing techniques in the evaluation of images obtained by visualizing the physical phenomena. General purpose image processing software is also available on the market, and it can significantly reduce the programming effort required for specific applications.

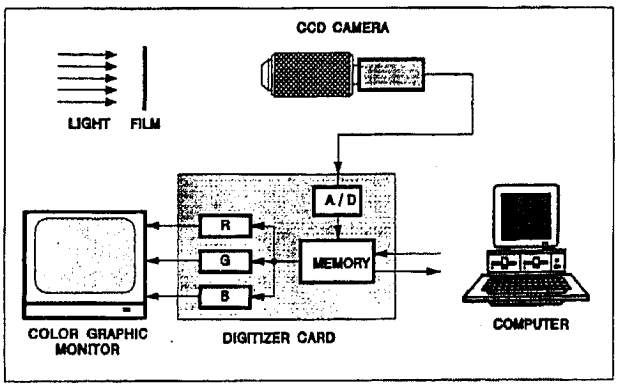

Fig. 2 Schematic of the setup for the evaluation of temperature fields recorded by a high-speed camera using a digital image processing system.

The configuration of the digital image processing system used in the evaluation process is presented in Fig. 2. In the high-speed, real-time measurements of temperature fields by holographic interferometry, interferograms are recorded on a 16 mm film, since commonly used video cameras cannot achieve the high velocities needed in these measurements. The developed film is positioned into a holder and transilluminated by a light source. The interferograms are then recorded by a video camera connected to a digitizer card in a personal computer. The images are digitized with a spatial resolution of 768 X 512 pixels. The information on light intensity is coded digitally as 256 grey levels. The digitized image can then be observed on a high-resolution screen.

A commercially available digital image processing software package (Bioscan Optimas Version 2.03) is used as the basis for the development of the software for our specific application. It enables the recording of the digitized images and manual setting of the marker flags, and it supports basic filtering operations to improve image quality as well as the generation of overlays. Data on pixel coordinates as well as the digitized intensity values can be exported for further evaluation. An Optimas specific programming language, similar in structure to the C language, allows for the development of application specific programs which can be combined with the basic program package.

The first step of the algorithm for our specific application is the determination of the position of the walls and the position of the heated plates. Marker flags are set in the wall region at the point of transition from minimum to maximum light intensity (the transition from dark to light tones is less steep in the case of the isotherms). The program allows for an interactive correction of the markers. By means of linear interpolation, equations of the straight lines describing wall and plate contours are determined.

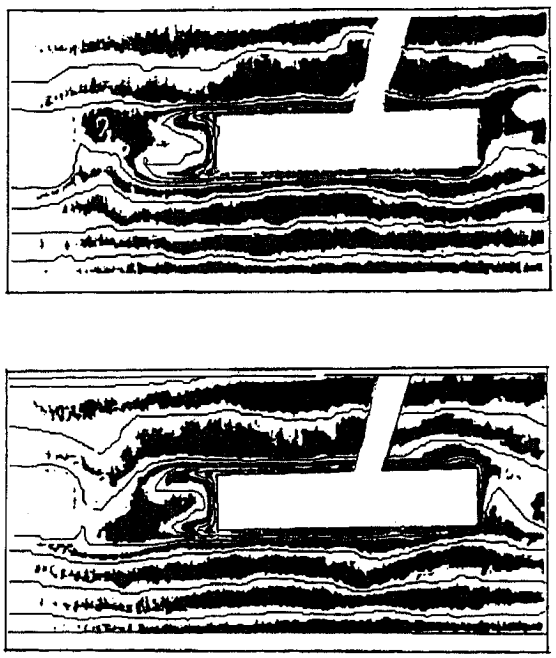

Fig. 3 Holographic interferograms recorded at two time instants visualizing the instantaneous temperature fields in the communicating channels and the superimposed overlay obtained by the data reduction procedure.

After defining a suitable coordinate system, the data reduction procedure begins. The lines corresponding to minimum and maximum intensity are traced along each isotherm. The results of the tracing procedure are illustrated in Fig. 3. The set of lines obtained in this way is then stored separately in the form of an overlay. The wall determination and the isotherm tracing procedures are repeated for the desired number of images and the data are stored. Color coding helps to distinguish between the different superimposed images. Thermocouple measurements at two distinct points in the field of view have shown that the uncertainty in the temperature calculations for the individual interferograms is in the range of 2-3%.

In the following step, the desired number of overlays, (which usually is not more than four to avoid loss of detail in

the overcrowded picture) are placed over each other to observe the changes of the transient phenomenon in the investigated time interval.

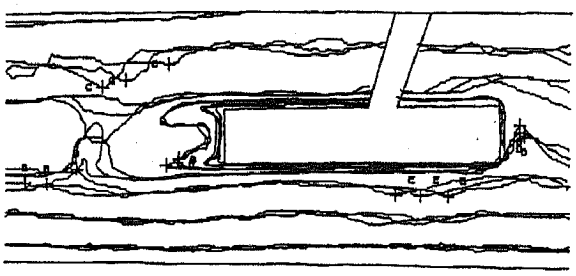

Fig. 4 Four superimposed overlays obtained in the evaluation of an interferogram sequence.

Particular events can be selected such as the setting of marker flags to identify the motion of a specific point between the individual expositions, as indicated in Fig. 4, where **A** refers to the location of the maximum of the isotherm extreme in the vortex region, **B**, the propagation of a characteristic maximum in the bottom channel region, **C**, the propagation of a characteristic minimum in the top channel region, **D**, the characteristic maximum in the region of the leading edge of the heated plate, and **E**, the propagation of a characteristic minimum in the bottom channel region. Due to the complexity of the analyzed process, these markers are set manually, as the judgement of the operator in identifying the characteristic points of a set of images is essential. For the investigated physical situation, automatic data processing is not possible. The coordinates of the marked events can be exported to data files which are then subject to further evaluation. In this way, wavelength and propagation velocity of the travelling waves and the frequency of the thermal oscillations in different regions of the communicating channels can be measured. The evaluation procedure can be easily modified and adjusted to consider different geometries and different physical situations.

Figure 5 shows a temporal sequence of holographic interferograms recorded at a Reynolds number of 593 by high-speed cinematography at a velocity of 600 frames per second. From the sequence of interferograms, the velocity of wave propagation and the wavelength can be determined by measuring the locations of wave minima and maxima. The oscillation amplitudes of the isotherm extreme in the vortex region obtained by using the digital image processing technique described above for the sequence of interferograms in Fig. 5 are shown in Fig. 6.

Numerical Simulations and Computer-Aided Animations

In this section, a series of numerical simulations are presented for the geometry described earlier. The parameter that is varied in the numerical simulations is the Reynolds number which is based on the channel half-height and the cross-channel average velocity. The Reynolds number ranges from 150 to 300.

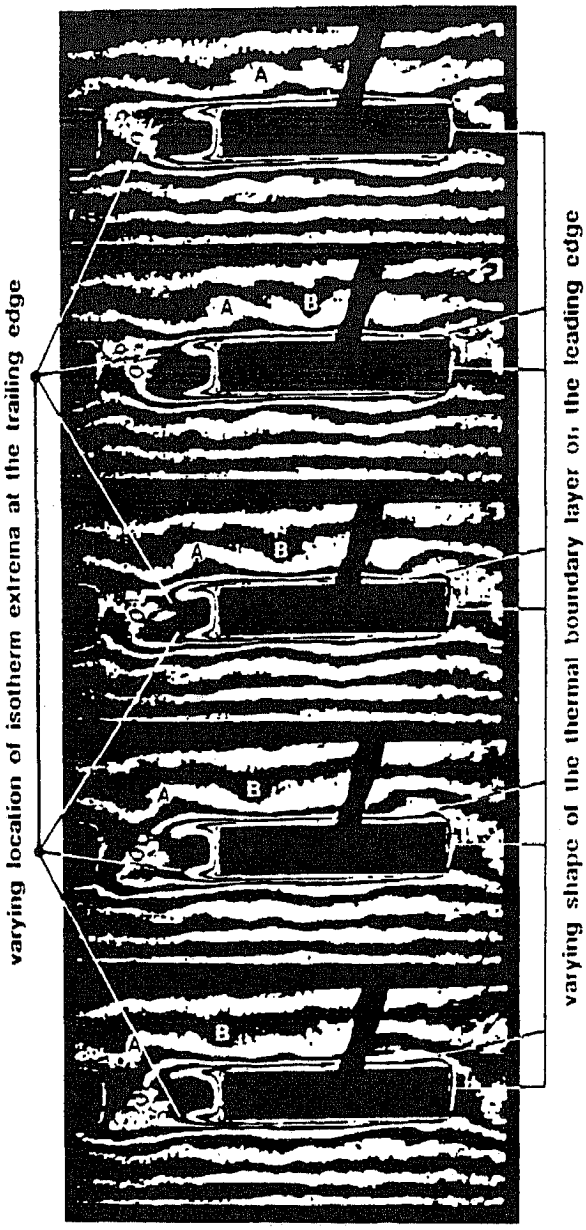

(A) maximum of the traveling wave

(B) minimum of the traveling wave

Fig. 5 Temporal sequence of holographic interferograms at Reynolds number of 593 recorded at 600 frames per second.

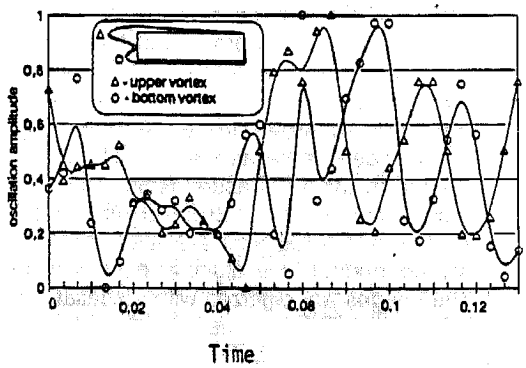

Fig. 6 Amplitudes of isotherm extreme in the vortex region versus time at Reynolds number of 593; Δ upper vortex, o bottom vortex.

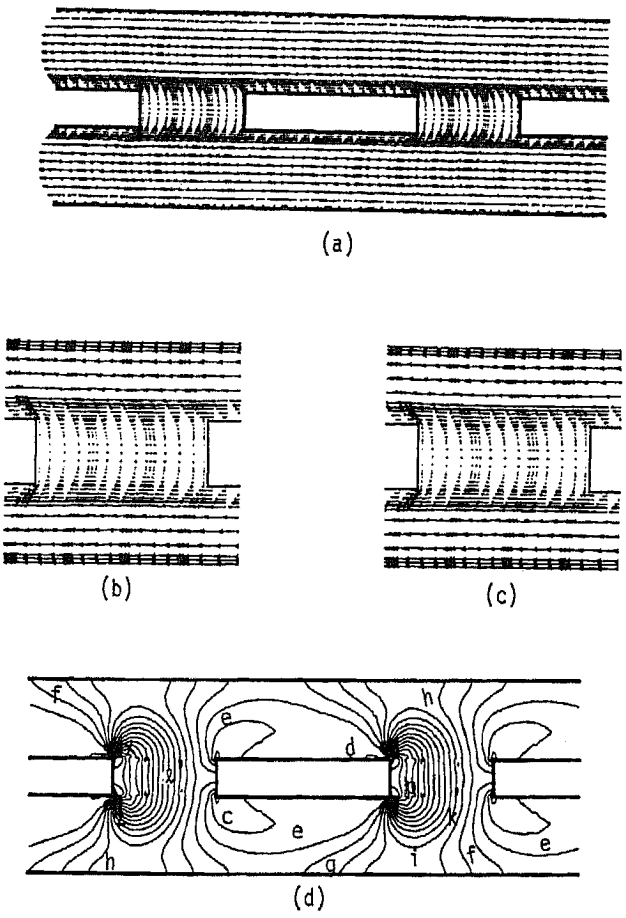

Fig. 7 a) Instantaneous velocity field at Reynolds number of 150; b) and c) Magnified communicating regions of the left and right sides, respectively; d) Instantaneous isobars equally spaced from $a=p_{min}$ to $z=p_{max}$.

Figures 7-9 indicate instantaneous velocity vector fields, the associated zoomed-in communicating regions and the pressure fields for Reynolds numbers of 150, 250 and 300, respectively. Looking at the magnified communicating regions (Figs. 7(b) and (c)) on either side of the velocity vector fields of Fig. 7(a), one can see that there are two vortices rotating in opposite directions that are aligned and confined to the communicating regions, a phenomenon that can be attributed to strong viscous effects present in low Reynolds number flows (Amon and Mikic, 1990). The flow field is steady at this Reynolds number of 150. The corresponding pressure contours are shown in Fig. 7(d). The high pressure zones are on the vertical wall near the leading edges of the interrupted plates. A close look at the velocity vector fields of either Fig. 7(b) or (c) reveals that near these regions the oncoming flow is stagnant, which results in high values of pressure. Increasing the value of the Reynolds number unsettles the vortices and disrupts the steady state of the flow and, at a Reynolds number of 250 (Fig. 8), the flow is seen to have already become oscillatory in nature. The vortices communicate with the main flow regions inducing a better flow mixing. Figure 9 corresponds to a Reynolds number of 300 where the instantaneous flow field is seen to be much more oscillatory and the phenomenon of ejection of the vortices into the main-flow regions more pronounced. Figures 8 and 9, along with their respective blown-up communicating regions, reveal an interesting feature associated with the structure of the flow field and its dependence on the Reynolds number.

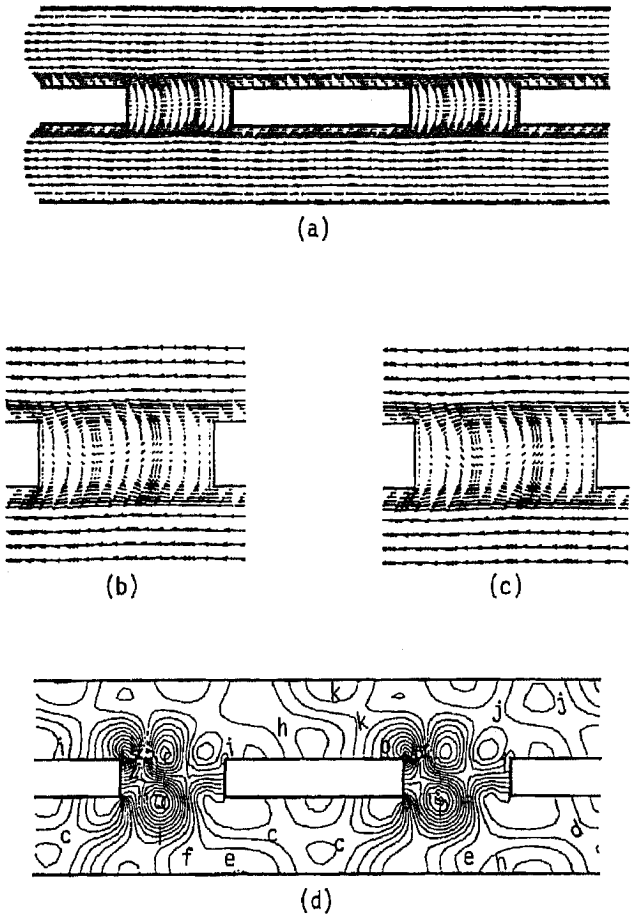

Fig. 8 a) Instantaneous velocity field at Reynolds number of 250; b) and c) Magnified communicating regions; d) Instantaneous isobars equally spaced from $a=p_{min}$ to $z=p_{max}$.

For a Reynolds number of 250 (Fig. 8), the vortical structures in the two communicating regions are identical, rotating in the same direction; whereas, for a Reynolds number of 300 (Fig. 9), the two vector fields are antisymmetric and the vortices are ejected in a staggered fashion to the upper and the lower channels. These phenomena can be observed in the corresponding instantaneous pressure fields as well. For example, in Fig. 8(d), the pressure fields in the communicating regions are almost identical whereas in Fig. 9(d), they are antisymmetric. The visualization of the instantaneous velocity and pressure fields indicates a strong correspondence between the stagnation flow and the high-pressure region.

The high-pressure regions in the instantaneous pressure contours of Fig. 8(d) are near the upper end of the vertical wall at the leading edge where the flow impinges upon, creating a local stagnation flow as seen in Fig. 8(a). Similar correspondence between the instantaneous velocity and pressure fields is observed in Figs. 9(a) and (d). The flow structure in the communicating regions is also in agreement with the traveling wave structure in the main channels. Therefore, the vortical structures in two consecutive communicating regions are identical when an even number of traveling waves spans the double geometric periodicity

length for a Reynolds number of 250, whereas, the vortical structures are antisymmetric when an odd number of waves is present as in the case of Reynolds number equal to 300.

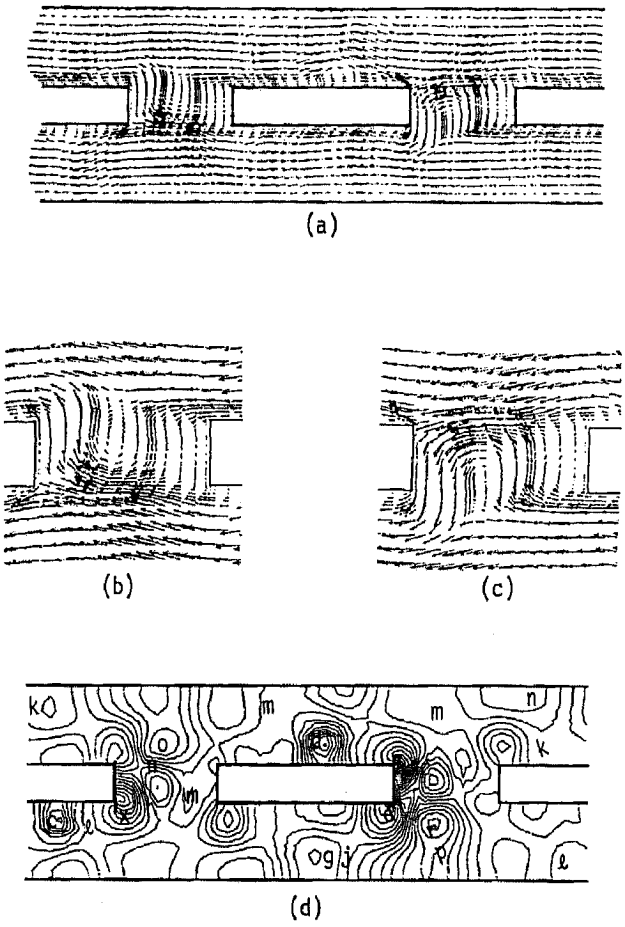

Fig. 9 a) Instantaneous velocity field at Reynolds number of 300; b) and c) Magnified communicating regions; d) Instantaneous isobars equally spaced from $a=p_{min}$ to $z=p_{max}$.

Upon analyzing the frequency of the oscillatory velocity components by performing a Fourier analysis, these traveling waves are found to be Tollmien-Schlichting-like in nature (Amon et al., 1991). In fact, for a certain range of Reynolds numbers, we found the presence of a single dominant Fourier frequency. The frequency is non-dimensionalized by the convective time which is the time necessary for a fluid particle traveling with the velocity at the midplane of the main channel to move the half-channel height distance. For a Reynolds number of 250 and the geometry under consideration, the nondimensional angular frequency is 0.7504 which corresponds to 24.97 Hz. This frequency closely matches the Tollmien-Schlichting frequency of 0.8098 obtained from the solution of the Orr-Sommerfield equation.

Another interesting observation can be made from the high Reynolds number flow field of Fig. 9. The flow is seen to have separated from the walls of the interrupted plates, which is a consequence of the relatively high amplitude of the oscillations that results in localized adverse pressure gradients.

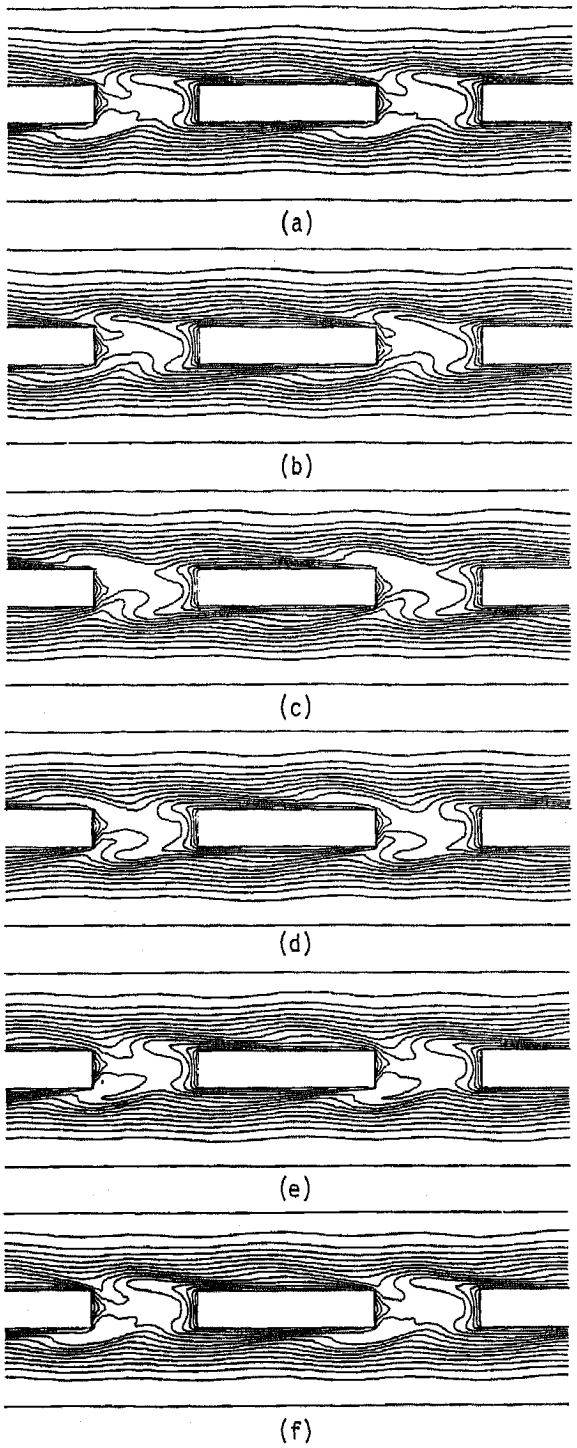

Fig. 10 Instantaneous isotherm plots at Reynolds number of 250 in one time-period T of the flow cycle at time instants a) T/10, b) 3T/10, c) 5T/10, d) 7T/10, e) 9T/10 and f) T.

Instantaneous isotherm plots for a Reynolds number of 250 are shown in Figs. 10(a-f) as a sequence of six time-frames within one flow cycle of time period T=0.04 second. One flow cycle corresponds to the time in which the velocity at a fixed point undergoes a complete oscillation about a mean value. The temperature fields show the waviness of the flow more clearly than the velocity vector plots. In this sense, the temporal sequence of isotherms is a thermal visualization of the Tollmien-Schlichting waves present in the main channels. A close look at the plots confirms that an even number of traveling waves spans the geometric length at this Reynolds number of 250. The sequence of temperature fields reveal another phenomenon worth

mentioning. If a typical isotherm in one of the communicating regions of Fig. 10(a) is selected, and its evolution followed up in time through the flow cycle (Figs. 10(a-f)), it is found that by the time the thermal traveling wave traverses half of one periodicity length, the growth and decay of the isotherm undergoes a complete periodic cycle. Thus, there exists a correspondence between the frequency of the decay and growth of the isotherms in the communicating regions and the speed of the traveling waves in the main channels. It is also interesting to note the thickening and thinning of the boundary layers as the flow turns at the trailing edges of the interrupted walls.

An animation graphics technique is used to facilitate the visualization of the time-varying temperature fields. All computed results are converted into a series of frame images using a package of subroutines called DrawCGM available at the Pittsburgh Supercomputing Center, which can directly create a CGM metafile. Thirty frames are used to produce a computer-aided animation for one second. The highlight of the present numerical work is a videotape displaying, in real time, the evolution of the temperature field in two complete cycles of the self-sustained oscillatory flow, starting from a state determined to be convergent in time. One second of real-time video represents 0.3 units of dimensionless time which is non-dimensionalized by the convective time.

Conclusion

A combined experimental and numerical investigation in communicating channels was performed to gain more insight into the physics of oscillatory thermo-fluid phenomena. The results of the visualizations using numerical animation show good agreement with the experimental visualizations of the temperature fields using holographic interferometry. The data reduction procedure developed for the experimental evaluation of transient temperature fields in the communicating channels enables easy qualitative and quantitative comparisons of interferograms recorded at different time instants. This is achieved by reducing the amount of information contained in the individual images where the operator can select and mark characteristic events and store only the corresponding relevant quantitative data. The flow structures and pressure fields in the communicating regions are in agreement with the traveling wave structure. The frequencies of the growth and decay of the isotherms in the communicating regions correspond to the frequency of the self-sustained oscillatory flow and are related to the speed of the traveling waves in the main channels.

Acknowledgments

Support by the National Science Foundation under Grants CTS-8908808 and ECD-8943164 is gratefully acknowledged.

References

Amon, C. H. and Mikic, B. B., 1990, "Numerical Prediction of Convective Heat Transfer in Self-Sustained Oscillatory Flows," *J. Thermophysics and Heat Transfer*, 4(2) pp. 239-246.

Amon, C. H., Herman, C. V., Majumdar, D., Mayinger, F., Mikic, B. B. and Sekulic, D., 1991, "Numerical and Experimental Study of Self-Sustained Oscillatory Flows in Communicating Channels," To appear in *Int. J. Heat Mass Transfer.*

Bareta, J. M., 1991, "Numerical Visualization of Complex Flows," *ASME* FED-Vol. 128, pp. 343-346.

Buning, P. G. and Steger, J., 1985, "Graphics and Flow Visualization in Computational Fluid Dynamics," *AIAA* Paper 85-1507CP.

Herman, C. V. and Mayinger, F., 1991, "Interferometric Study of Heat Transfer in a Grooved Geometry," *Proc. 2nd World Conference on Experimental Heat Transfer, Fluid Mechanics and Thermodynamics*, June 23-28, 1991, Dubrovnik, Yugoslavia, Eds. J. F. Keffer, R. K. Shah and E. N. Ganilic, Elsevier, New York, pp. 522-529.

Herman, C. V., Mayinger, F. and Sekulic, D. P., 1991, "Experimental Verification of Oscillatory Phenomena in Heat Transfer in a Communicating Channels Geometry," *Proc. 2nd World Conference on Experimental Heat Transfer, Fluid Mechanics and Thermodynamics*, June 23-28, 1991, Dubrovnik, Yugoslavia, Eds. J. F. Keffer, R. K. Shah and E. N., Ganilic, Elsevier, New York, pp. 904-911.

Hesselink, L., 1988, "Digital Image Processing in Flow Visualization," *Ann. Rev. Fluid Mech.*,Vol. 20, pp. 421-485.

Hunter, J. C. and Collins, M. W., 1987, "Holographic Interferometry and Digital Fringe Processing," *J. Phys. D: Appl. Phys.* 20, pp. 683-691.

Merzkirch, W., 1987, Flow Visualization, Academic Press, Orlando.

Osten, W., Saedler, J. and Rottenkolber, H., 1987, "Quantitative Auswertung von Interferogrammen mit einem digitalen Bildverarbeitungssystem," *Technisches Messen,* Vol. 54, No. 7/8, pp. 285-290.

Patera, A. T., 1984, "A Spectral Element Method for Fluid Dynamics: Laminar Flow in a Channel Expansion", *J. Computational Physics*, Vol. 54, pp. 468-488.

Van Dyke, M., 1982, An Album of Fluid Motion, Parabolic Press, Stanford, California.